IOP Conference Series:
Earth and
Environmental Science

PURPOSE-LED PUBLISHING™

PAPER • **OPEN ACCESS**

Effects of Grain Shape Angularity on Cohesive Strength in Sheared Granular Media

To cite this article: T. Binaree *et al* 2025 *IOP Conf. Ser.: Earth Environ. Sci.* **1480** 012042

View the article online for updates and enhancements.

You may also like

- Recent outreach activities of the EEE Project
C. Ripoli, M. Abbrescia, C. Avanzini et al.
- Ellipsometry Analysis of Titanium Nitride Thin Film Prepared by Reactive Magnetron Sputtering
Fanyu Meng, Hua Cai, Gang Yu et al.
- The Morphological Features of the Qitianling Granitic Pluton: Constrains from Magnetotelluric Data in Southern Hunan
Keke Zhou, Jianxin Liu, Li Cao et al.

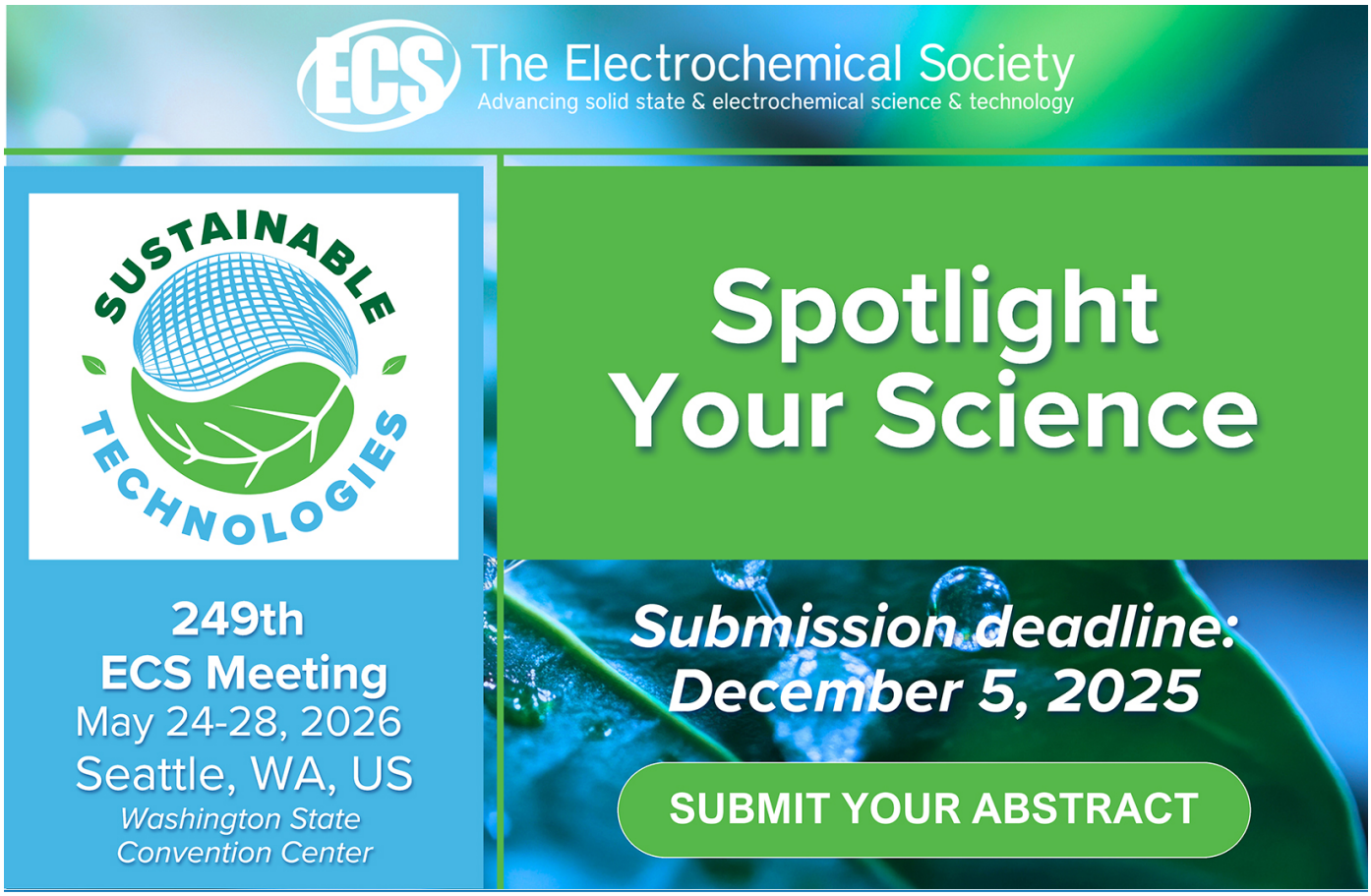

This content was downloaded from IP address 132.207.4.76 on 24/11/2025 at 19:35

IOP Conf. Series: Earth and Environmental Science **1480** (2025) 012042 doi:10.1088/1755-1315/1480/1/012042

EFFECTS OF GRAIN SHAPE ANGULARITY ON COHESIVE STRENGTH IN SHEARED GRANULAR MEDIA

***T. Binaree*[1], *P. Jitsangiam*[1], *M. Renouf*[2] *and E. Azéma*[2,3,4]✉**
[1] *Chiang Mai University-Advanced Railway Civil and Foundation Engineering Center (CMU-RailCFC), Department of Civil Engineering, Faculty of Engineering, Chiang Mai University, 239 Huay Kaew Road, Muang, Chiang Mai, 50200, Thailand*
[2] *LMGC, Université de Montpellier, CNRS, Montpellier, France*
[3] *Department of Civil, Geological and Mining Engineering, Polytech. Montréal, Montréal, Canada.*
[4] *Institut Universitaire de France (IUF), Paris, France*
✉ *emilien.azema@umontpellier.fr*

Abstract: Using extensive Contact Dynamics simulations, we present a systematic analysis concerning the effects of particle shape angularity on the quasi-static shear strength properties of cohesive granular packings under biaxial conditions for various confining stresses σ_0. We consider irregular polygons with an increasing number of sides, ranging from triangles to discs. The packings behavior depends on the dimensionless Cohesive Index $\eta = f_0/(\sigma_0 d)$, where f_0 is the contact adhesive force and d is the mean grain diameter. η is varied between 0 (dry) to 0.6 (strongly cohesive) by varying σ_0. We find that the macroscopic friction angle increases with grain angularity and saturates at larger angularity, as in the dry case. In contrast, the cohesive strength is an increasing function of grain angularity. Our results contribute to a better understanding of the effects of grain shape on the behaviour of cohesive granular materials, by complementing a number of results obtained mainly in the dry case.

1. Introduction

In granular materials, cohesive interactions among particles play a pivotal role in influencing the macroscopic behavior of the material. The importance of cohesive granular media extends to a variety of fields, underpinning crucial aspects of particle processing, soil mechanics and powder technology [1]. In the specific case of railway ballast, the presence of fine particles (resulting from the gradual degradation of the grains), combined with external agents (infiltration of water, silt, clay, climate variation), contribute to accelerate the deterioration of the ballasted track. These fine materials then act as a binder, causing the larger particles to stick together, drastically altering the stability characteristics of the ballasted track [2].

Extensive research has been carried out on wet or cohesive granular materials in various theoretical frameworks, based on experimental tests and/or numerical simulations [3, 4, 5]. In general, local cohesive forces f_0, regardless of their origin, confer an additional cohesive strength c (also termed *"Coulomb cohesion"*) to granular materials, supplementing the inherent frictional strength $\sin\varphi$, where φ denotes the macroscopic friction angle under dry conditions [1]. However, the bulk of existing studies on cohesive or wet granular media have primarily utilized circular (in 2D) or spherical (in 3D) particles. Real-world grains, however, exhibit irregular, elongated, or non-convex shapes, potentially establishing multiple points of contact, thereby augmenting the overall interparticle cohesive forces. This increase in geometrical/mechanical constraints, in turn, increases the cohesive and frictional strength of the system by preventing particle rotations. In the context of railways ballast, considering a realistic grain shape assumes even greater importance for enhancing track design, maintenance strategies, and the overall performance of railway systems.

It is now fairly well documented in the literature how the frictional resistance can change, often in a non-linear manner, as the grain shape varies from that of a disc to very angular or very elongated

Content from this work may be used under the terms of the Creative Commons Attribution 4.0 licence. Any further distribution of this work must maintain attribution to the author(s) and the title of the work, journal citation and DOI.
Published under licence by IOP Publishing Ltd

grains [7, 8, 9, 10]. On the other hand, the effect of grain shape on cohesive strength has not been widely studied. In this article, a systematic numerical investigation is presented on the effects of particle shape angularity on the quasi-static shear strength properties of cohesive granular packings under biaxial conditions for various confining stresses. Irregular polygons with an increasing number of sides, ranging from triangles to discs, together with a constant local adhesive force f_0 acting at contact points are considered in the study.

2. Numerical Setup

The study explores particle shapes, focusing on discs and polygons with sides (n_s) in the set $\{20, 10, 8, 7, 6, 5, 4, 3\}$. We define the angularity parameter α from the number of sides by $\alpha = 2\pi/n_s$, which varies from 0 (discs) to ~ 2.09 (triangles). Samples were prepared following a standardized protocol. Using a geometrical layer-by-layer deposition technique, 10 000 discs were densely packed within a rectangular box. To prevent long-range ordering, a small-sized polydispersity was introduced by varying particle diameters within a specified range [d_{min},d_{max}], where d_{max}=$1.25d_{min}$. Then, discs were substituted with angular particles with random orientation. After this geometrical process, an isotropic compression is imposed by applying a constant normal stress to all walls. During this stage, friction between grains and between grains and walls are set to 0. The gravity is also set to 0 in order to avoid force gradients. Snasphots of some of the packings at the end of isotropic compression are shown in Fig. 1. Then, friction between grains is set to 0.3, and the isotropic samples are sheared in

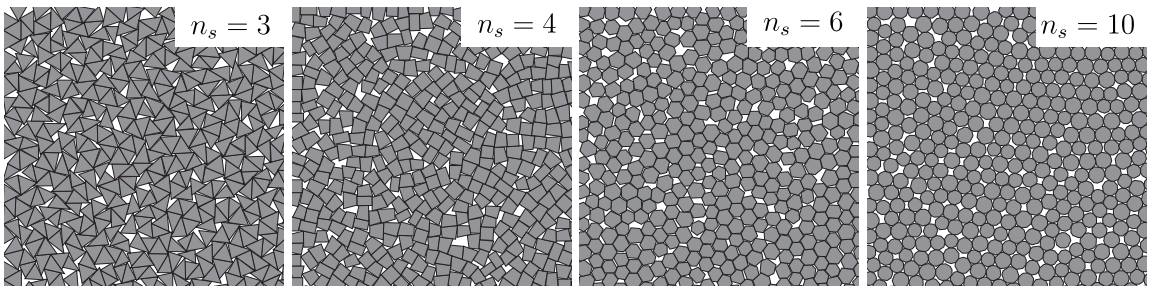

Figure 1. Some examples of samples after isotropic compression.

bi-axial compression by applying a constant velocity on the top wall and a local stress σ_0 on the two lateral walls. The local adhesion is activated to a constant value of f_0. In this condition, the relevant dimensionless parameter is the so-called "Cohesion Index" defined as $\eta = f_0/(\sigma_0 d)$ [3, 6], which is varied in the range $\eta \in [0, 0.01, 0.05, 0.1, 0.15, 0.2, 0.3, 0.4, 0.5, 0.6]$ for each value of α. Finally, it is worth mentioning that we focus on the quasi-static behavior and thus the so-called "inertial number" I remains below 10^{-3} for all simulations [11].

For the simulations, the Contact Dynamics (CD) method, a class of discrete element method (DEM), is utilized with irregular polygonal particles [12]. The method is incorporated within the LMGC90 platform, a multipurpose software developed in Montpellier. It should be noted that in CD, side-side are treated as 2 distinct contact points and thus, only the resultant of forces is physically significant. Consequently, a side-side contact exhibit a tensile strength that is 2 times greater than a side-vertex contact.

3. Numerical Results

As an illustration, Fig. 2 displays the evolutions of the stress ratio q/p as a function of the vertical deformation ε_1 for packings composed of irregular pentagons and increasing η (a), and for $\eta = 0.3$ and different grain angularities (b). Both, the q-deviator stress and the mean normal stress

p are defined from the principal values of the granular stress tensors, σ_1 and σ_2, respectively, as $q = (\sigma_1 - \sigma_2)/2$ and $p = (\sigma_1 + \sigma_2)/2$. As we can see, the stress-strain curves follow general trends as classically observed in the literature: a stress peak at low strains, followed by a decrease that spreads out until a constant phase where q/p evolves slightly around its mean value. This is the residual state known in soil mechanics, which is independent of the initial state. On these two examples we can also notice that the shear strength increases with both η and α. In the following, the reported quantities correspond to the mean values in the steady state (where $\varepsilon_1 > 0.25$). The cohesive strength c^* and

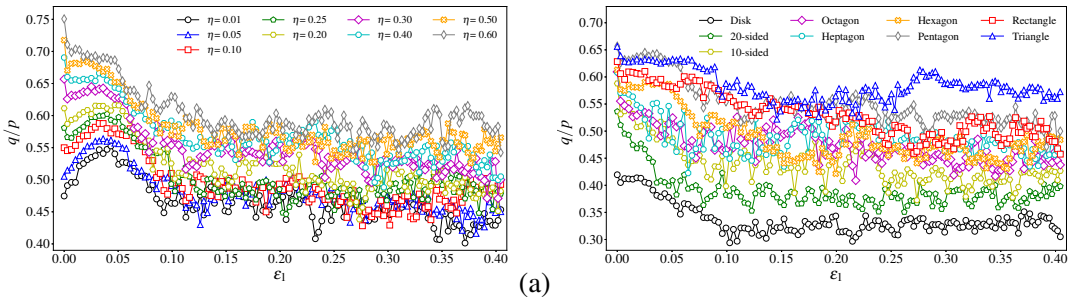

(a) (b)

Figure 2. Evolution of the stress ratio q/p as functions of the vertical strain ε_1: (a) packings of pentagons for all values of cohesion number η, (b) packing with $\eta = 0.3$ for all shapes.

the macroscopic friction φ^*, at residual state, can be deduced from Mohr-Coulomb relation, which predicts a linear relation between q^* and p^* (the averaged values of q and p in the residual state) as follows:

$$q^* = \sin\varphi^* p^* + c^* \cos\varphi^*. \tag{1}$$

As it can be seen from Fig.3(a), Eq. 1 is perfectly verified for all the α values simulated in this work. In particular, we observe that the increase of q^* with p^* is faster (*i.e.,* the slope of the line increases) as the angularity of the grains increases.

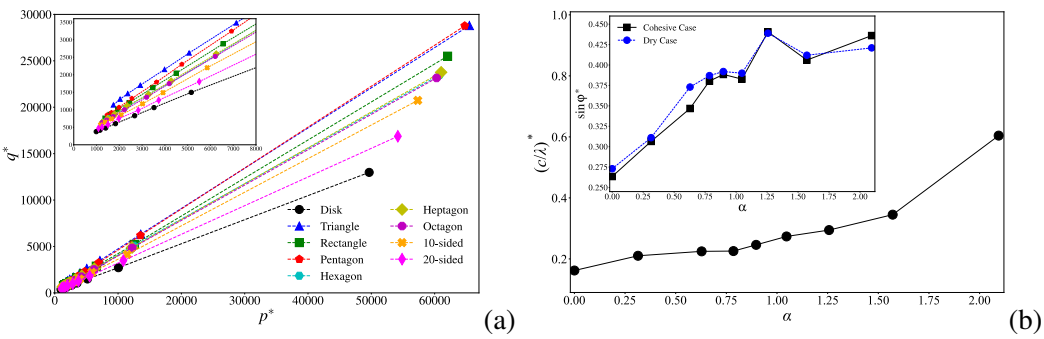

(a) (b)

Figure 3. (a) Mohr-Coulomb diagram showing the mean deviator stress q^* as a function of mean stress p^* (both averaged in the residual state) for all α and a zoom shows at low pressures (inset), (b) Residual state normalized cohesive strength c^*/λ and residual state macroscopic friction angle $\sin\varphi^*$ (inset), both as a function of particle angularity α.

Figure 3(b) displays the variations of the residual state macroscopic friction angle $\sin\varphi^*$ (inset), as well as the residual state normalized cohesive strength c^*/λ, where $\lambda = f_0/d$, both as a function of the angularity α. As we can see, $\sin\varphi^*$ increases with the angularity of the grains and tends to saturate

at the highest values of α. These trends are consistent with previous results obtained in the dry case [8, 10] and as expected, the $\sin\varphi^*$ values measured in the cohesive case (black lines/symbols) are very close to those measured in the dry case (blue lines/symbols). On the other hand, we find that the macroscopic cohesion c^* is an increasing function of the angularity α, even though the local cohesion f_0 is identical for each simulated system. In other words, grain angularity enhances the cohesive strength of granular materials.

4. Conclusion

This study employs extensive Contact Dynamics simulations to systematically analyze the combined effects of grain angularity and contact cohesion on the frictional and cohesive strength of sheared granular assembly. Irregularly shaped polygons are considered by systematically varying their number of sides from triangles to 20-sided polygons and discs. A basic result of the study presented here is that cohesive strength increases as grain angularity increases. The results we present, which are preliminary at this stage, suggest a subtle link between grain shape (a geometric property) and macroscopic cohesion (a mechanical property). In this sense, our results open the door for a better understanding of the effects of grain shape on the behaviour of cohesive granular materials, complementing a number of results obtained mainly in the dry case, or in the cohesive case but with spherical grains.

This research is supported by the Franco-Thai Young Talent Research Program, co-funded by the Embassy of France in Thailand and the NSRF via the Program Management Unit for Human Resources and Institutional Development, Research and Innovation [grant B13F660083].

References

[1] Andreotti, B., Forterre, Y., and Pouliquen, O. (2013). *Granular Media: Between Fluid and Solid*. Cambridge University Press.
[2] Trinh, V. N., Tang, A. M., Cui, Y.-J., Dupla, J.-C., Canou, J., Calon, N., Lambert, L., Robinet, A., and Schoen, O. (2012). Mechanical characterisation of the fouled ballast in ancient railway track substructure by large-scale triaxial tests. *Soils and Foundations*, **52**, 511–523.
[3] Khamseh, S., Roux, J.-N., and Chevoir, F. (2015). Flow of wet granular materials: A numerical study. *Physical Review E*, **92**, 022201.
[4] Gans, A., Pouliquen, O., and Nicolas, M. (2020). Cohesion-controlled granular material. *Phys. Rev. E*, **101**, 032904, publisher: American Physical Society.
[5] Wang, J., Yu, H. S., Langston, P., and Fraige, F. (2011). Particle shape effects in discrete element modelling of cohesive angular particles. *Granular Matter*, **13**, 1–12.
[6] Badetti, M., Fall, A., Chevoir, F., and Roux, J.-N. (2018). Shear strength of wet granular materials: Macroscopic cohesion and effective stress: Discrete numerical simulations, confronted to experimental measurements. *The European Physical Journal E*, **41**, 68.
[7] Azéma, E. and Radjaï, F. (2010). Stress-strain behavior and geometrical properties of packings of elongated particles. *Phys. Rev. E*, **81**, 051304.
[8] Azéma, E., Estrada, N., and Radjai, F. (2012). Nonlinear effects of particle shape angularity in sheared granular media. *Physical Review E*, **86**, 041301.
[9] Azéma, E., Radjai, F., and Dubois, F. (2013). Packings of irregular polyhedral particles: Strength, structure, and effects of angularity. *Physical Review E*, **87**, 062203.
[10] Binaree, T., Azéma, E., Estrada, N., Renouf, M., and Preechawuttipong, I. (2020). Combined effects of contact friction and particle shape on strength properties and microstructure of sheared granular media. *Phys. Rev. E*, **102**, 022901.
[11] GDR MiDi (2004). On dense granular flows. *The European Physical Journal E*, **14**, 341–365.
[12] Jean, M. (1999). The non-smooth contact dynamics method. *Computer Methods in Applied Mechanics and Engineering*, **177**, 235–257.